AN INVESTIGATION OF MICROSTRUCTURE AND HAZ MICROFISSURING OF

CAST ALLOY 718

X. Huang and M.C. Chaturvedi
Dept. of Mech. Eng, University of Manitoba
N.L Richards
Bristol Aerospace Ltd., Winnipeg, Manitoba, Canada

Abstract

The effect of microstructure on the HAZ of cast alloy 718 has been examined in this study. The microstructure of the base material in various heat-treated conditions (homogenized at temperatures ranging from 1036°C to 1163°C, double solution treated at 927°C/1hr + 927°C and aged at 760°C/5hrs + 650°C/1hr) has been analyzed using optical microscopy, Scanning Electron Microscopy (SEM) and Transmission Electron Microscopy (TEM). The weldability of variously heat-treated material was evaluated by measuring Total Crack Length (TCL) in sections taken from a bead-on-plate electron beam welds.

The secondary microstructural constituents observed in cast alloy 718 were Laves phase, MC carbides, MN nitrides and δ-Ni_3Nb. The volume fraction of Laves and Ni_3Nb phases decreased with increasing heat treatment temperature, while the amount of MC carbide (+nitride) did not change up to 1163°C. Solution heat treatment caused an increase in the amount of Ni_3Nb precipitates both, inter and intra-granular, relative to the homogenized state. Ageing increased the material's hardness through the precipitation of $\gamma''+\gamma'$.

With increasing homogenization heat treatment temperature, the TCL values decreased initially (from 1037°C to 1066°C) and then increased (from 1066°C to 1163°C). Boron grain boundary segregation was found to be closely related to the variation in the TCL. The TCL values after homogenization and solution treatments showed a similar trend. Ageing of the material caused an increase in the TCL values in all the specimens regardless of the homogenization temperature as compared to the only homogenization treated material; however, the minimum in TCL value observed at 1037°/1066°C did not occur in the homogenized and aged condition.

Superalloys 718, 625, 706 and Various Derivatives
Edited by E.A. Loria
The Minerals, Metals & Materials Society, 1994

Introduction

Alloy 718 was developed in the early 1960's to provide a possible solution for the superalloy welding problems due to its sluggish γ''-Ni_3Nb precipitation reaction, which minimizes the alloy's propensity to strain-age cracking. Unfortunately the presence of Nb made it susceptible to intergranular and interdendritic microffissuring in the weld heat affected zone (HAZ) of the as-cast alloy.

Alloy 718 was originally utilized in the wrought form, but with the development of investment casting technology, cast alloy 718 has found wide application as compressor and turbine frame components in aircraft engines[1]. In the past three decades, most of the research has been focused on the alloys welded in the wrought condition. This research suggests that grain boundary melting resulting from the constitutional liquation of Nb-rich MC carbides leads to HAZ cracking during the welding thermal cycle[2]. Microfissuring in this condition can be effectively controlled through reducing the grain size to ASTM<#6[3]. Cast alloy 718 exhibits higher susceptibility to microfissuring than the wrought alloy due to the presence of Laves phase, coarse grain size and heavy dendritic structure. The microstructural features of cast alloy 718 are, however, considerably different than those of wrought 718. Therefore the reasons for the observed microfissuring of wrought 718 may not apply to the cast alloy.

Recent research work on the problems of microfissuring in cast alloy 718 has been conducted by Baeslack et al[4], Thompson et al[5,6], Kelly[7,8] and Richards et al[9]. The results of Baeslack et al[4] showed weld HAZ liquation to result from the constitutional liquation of residual Laves phase that where part of the original as-cast structure. This liquation reaction initiated at a temperature well below that required for constitutional liquation of MC carbides, which led to an increased HAZ liquation and more severe sensitivity to microfissuring as compared to wrought alloy 718. Thompson et al examined the role of grain boundary chemistry on HAZ microfissuring[5]. They concluded that the intergranular chemistry influences the temperature dependence of the grain boundary liquid distribution and therefore determines if a liquid film is present when the residual welding stresses build up. Both bulk chemical composition and the heat treatment affect the grain boundary S, C, and Nb segregation which in turn influence the HAZ microfissuring. Kelly et al[7,8] studied the influence of several alloying elements including Nb, Mn, Co, Ta, Si, B and Fe. The concluded that microfissuring of welds in cast alloy 718 was primarily associated with B and was exacerbated by Nb and Fe. Investigation on the influence of electron beam welding parameters on the weldability of cast alloy 718 by Richards et al[9] showed that welding speed at a sharp focus is the most effective parameter in controlling the HAZ microfissuring.

The present communication describes the effect of various heat treatments, i.e., homogenization, solid solution and ageing, on the microstructure and HAZ microfissuring of cast alloy 718. The mechanism(s) of HAZ microfissuring has been discussed in terms of 1) the amount of low melting secondary phases, 2)grain boundary precipitation, 3)grain boundary segregation and 4)material's hardness.

Experimental Procedures

Cast alloy 718, whose chemical composition is given in Table I and was supplied by Precision Cast Corporation, Portland, Oregon, was used in this study. The material was specially investment cast into 1.6 cm x 8cm x 20cm blocks for experimental purposes.

Table I Chemical Composition of Alloy 718(wt%)

Ni	Cr	Fe	Co	Mo	Nb	Si	Mn
52.97	18.61	Bal.	0.09	3.06	5.01	0.16	0.03
Ti	Al	B	S	C	P	Mg	Cu
0.81	0.43	0.003	0.005	0.07	0.009	<0.001	0.02

Zr<0.005 and Hf<0.005

For the preliminary evaluation of microstructure and weldability, various heat treatments were selected with the homogenization temperature ranging from 1037°C to 1163°C, and solutionizing and ageing temperatures as specified in Table II.

Table II Heat Treatment Parameters

Homogenization : 1037°C/1hr, 1066°C/1hr, 1093°C/1hr, 1163°C/1hr
Homogenization and solution(ST) : 1037°C/1hr + 927°C/1hr + 927°C/1hr 1066°C/1hr + 927°C/1hr + 927°C/1hr 1093°C/1hr + 927°C/1hr + 927°C/1hr 1163°C/1hr + 927°C/1hr + 927°C/1hr
Homogenization and ageing 1037°C/1hr + 760°C/5hr F.C.* to 650°C/1hr 1066°C/1hr + 760°C/5hr F.C. to 650°C/1hr 1093°C/1hr + 760°C/5hr F.C. to 650°C/1hr 1163°C/1hr + 760°C/5hr F.C. to 650°C/1hr

*F.C.-Furnace cool at a rate of 55°C/hr

Bead-on-plate electron beam welding was carried out at a speed of 152cm/min using electron beam at 44kV and 79mA. The HAZ microfissuring susceptibility can be evaluated by total crack length (TCL), average crack length and maximum crack length. It has been observed when no external stresses are imposed, the variation in TCL and maximum crack length with heat treatment, grain size and weld morphology follows the same trend[10]. In this study, TCL was used and measured as previously reported[11].

Specimens for the evaluation of microstructure and HAZ microfissuirng were prepared by mechanical polishing and etching by Kalling's II reagent. The microstructures were evaluated using JEOL 840 SEM/EDS and JEOL 2000FX TEM/STEM. Quantitative analysis was conducted on a Leitz image analyzer using a point counting method.

Results

Microstructures:

The as-cast alloy was heavily segregated as shown in the SEM micrograph in Fig.1, with the interdendritic areas appearing dark and the dendritic areas bright. The composition of both areas was measured by SEM/EDS and is shown in Table III. It should be noted that Nb is strongly partitioned to the interdendritic areas, while Cr and Fe are depleted in the interdendritic area. The interdendritic areas are also slightly enriched in Si, Ti and Mo, however Ni does not show any partitioning. The back scattered electron SEM image of the as-cast alloy is shown in Figs.2 and 3. Various phases seen in these figures were identified using both SEM/EDS and their morphological nature. They consist of a γ-matrix, needle-like δ-Ni_3Nb (Fig.2), lamellar Laves phase (Fig.2), cubic Ti-rich M(C,N) (Fig.3) and irregular-shaped Nb-rich M(C,N) (Fig.3). The secondary phases were found to be mainly present in the interdendritic area.

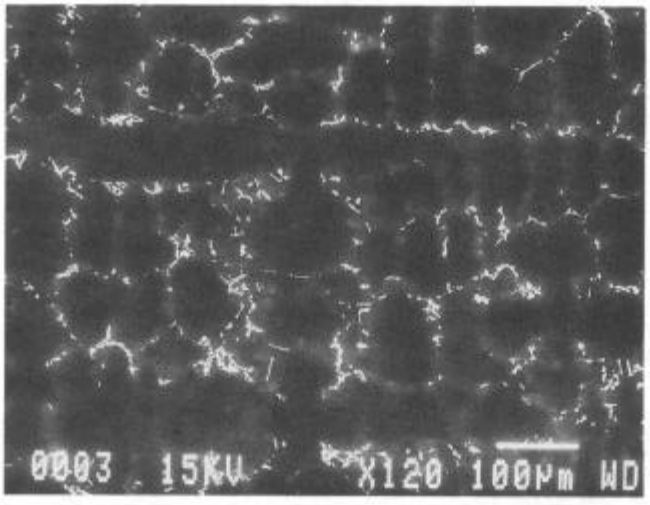

Fig.1 Microstructure of as-cast 718

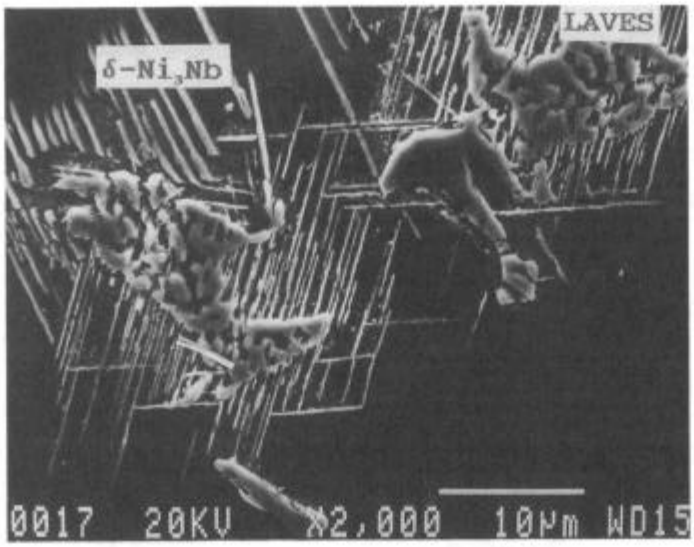

Fig.2 Microstructure of as-cast 718

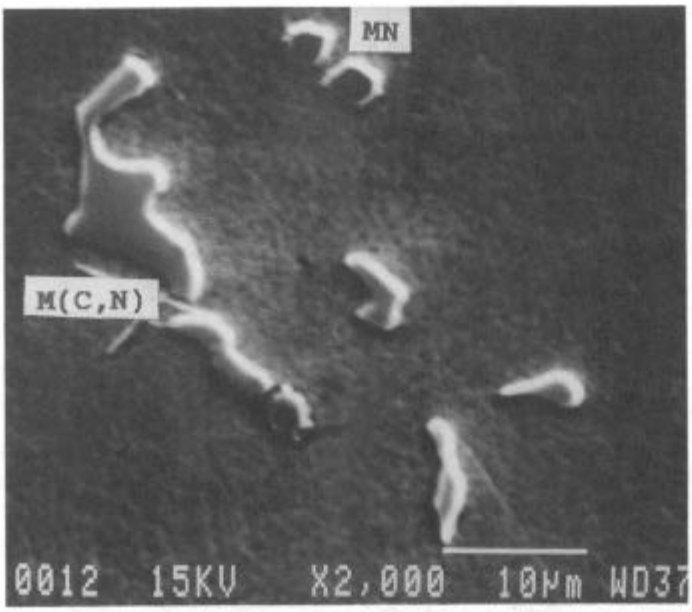

Fig.3 Microstructure of as-cast 718

The microstructure after homogenization treatment at 1037°C/1hr (Fig.4a) showed similar features as those observed in the as-cast condition, i.e., a γ-matrix, Ti-rich M(N), Nb-rich M(C,N) and Laves phase, but a smaller amount of δ-Ni3Nb phase. The microstructural examination of a specimen after the 1163°C/1hr heat treatment indicated that the δ-Ni3Nb had completely dissolved, as seen in Fig.4b; In addition, the Laves phase was hardly detectable after heat treatment at 1163°C for one hour, however, no change in the total amounts of Nb(C,N) and TiN was observed. Quantitative analysis (Figs.5a, 5b and 5c) showed that both δ (Fig.5a) and Laves phases (Fig.5b) decreased with increasing solid solution treatment temperature, while the amount of M(C,N) + MN (Fig.5c) remained constant.

The microstructure after solid solution treatment contains similar features as those observed in the homogenized condition when the microstructure of a specimen treated at 1037°C/1hr (Fig.4a) is compared with that of the material given a heat treatment of 1037°C/1hr + 927°C/1hr + 927°C/1hr (Fig.6). An increased amount of δ precipitates was observed after solutionizing, which is evident in Fig.5a. It was also found that most of the grain boundaries after solution treatment were covered by δ-Ni3Nb precipitates.

Table III Chemical Composition of Dendritic and Interdenditic Areas(wt%), SEM/EDS

	Interdendritic area			Dendritic area		
	Ave.	Max.	Min.	Ave.	Max.	Min.
Al	0.41	0.54	0.13	0.56	0.73	0.44
Si	0.43	0.86	0.27	0.27	0.37	0.15
Ti	1.38	1.85	1.10	0.48	0.60	0.38
Cr	15.04	18.56	8.41	20.1	20.27	19.78
Fe	13.95	17.35	7.36	20.8	21.55	19.65
Ni	51.47	54.55	48.39	52.3	52.96	52.05
Nb	13.88	24.86	7.41	2.7	3.76	2.07
Mo	3.34	4.60	2.64	2.88	4.08	2.54

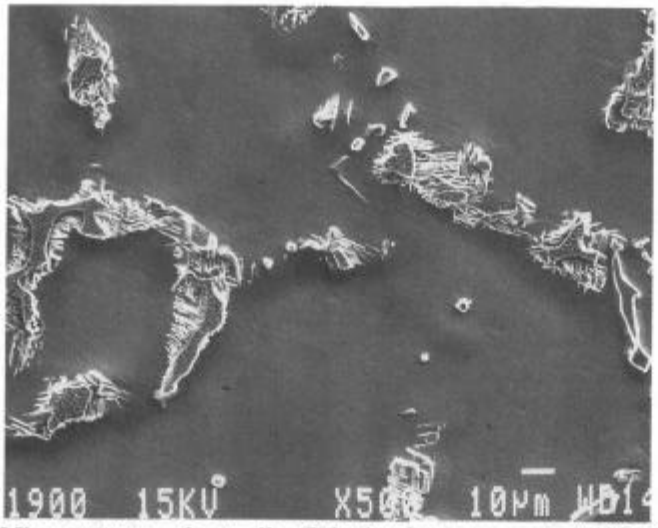

Fig. 4a Microstructure of cast alloy 718 after heat treament at 1037°C/ 1hr

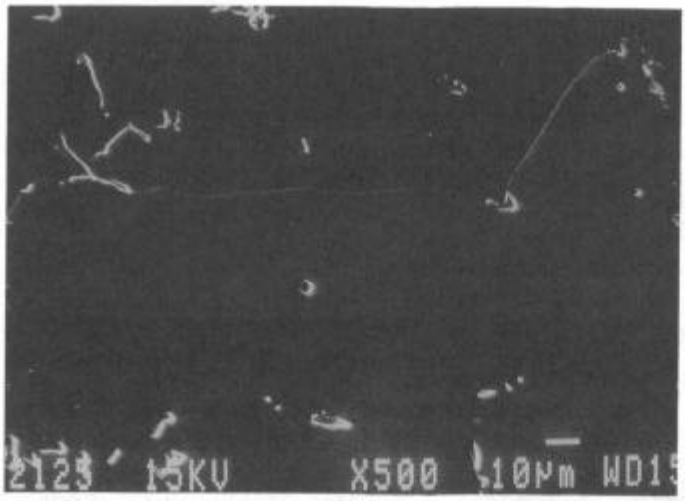

Fig.4b Microstructure of cast alloy 718 after heat treatment at 1163°C/ 1hr

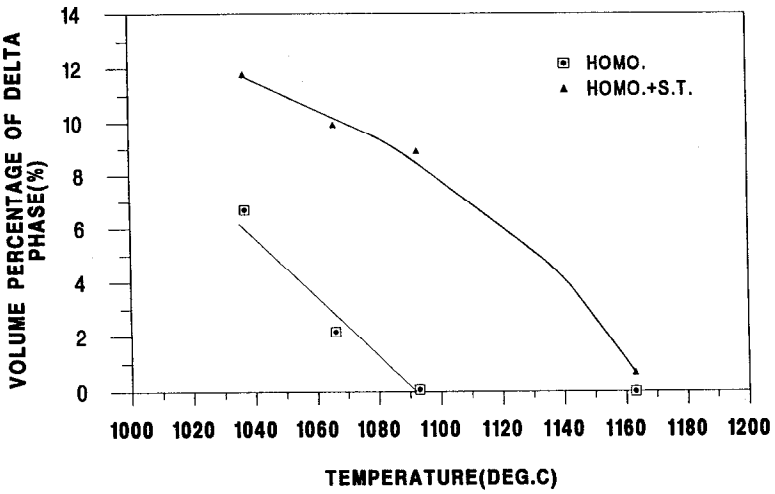

Fig.5a Effect of homogenization and solution heat treatment on the volume percentage of Ni3Nb phase

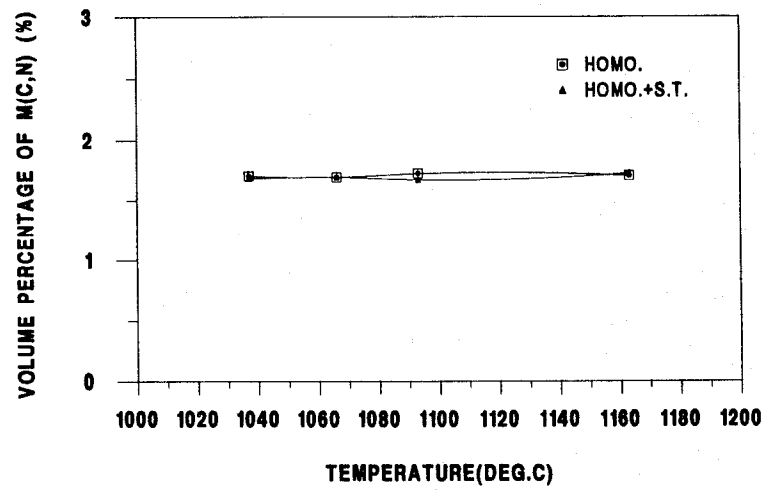

Fig.5b Effect of homogenization and solution heat treatment on the volume percentage of Laves phase

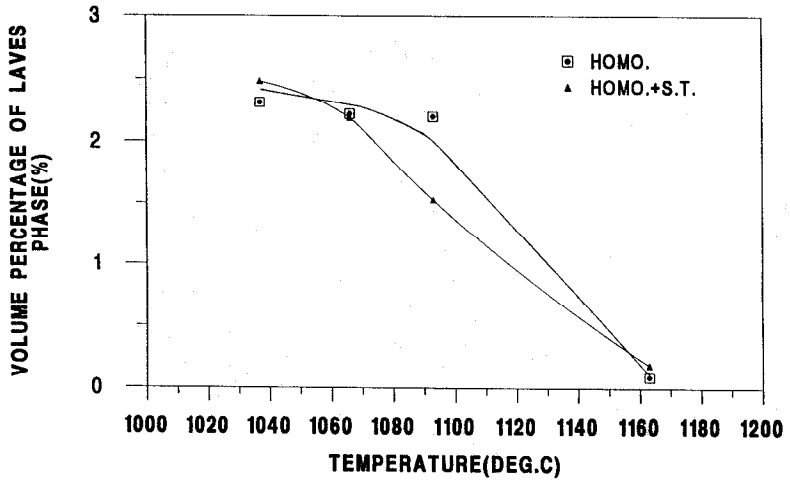

Fig.5c Effect of homogenization and solution heat treatment on the volume percentage of M(C,N) phase

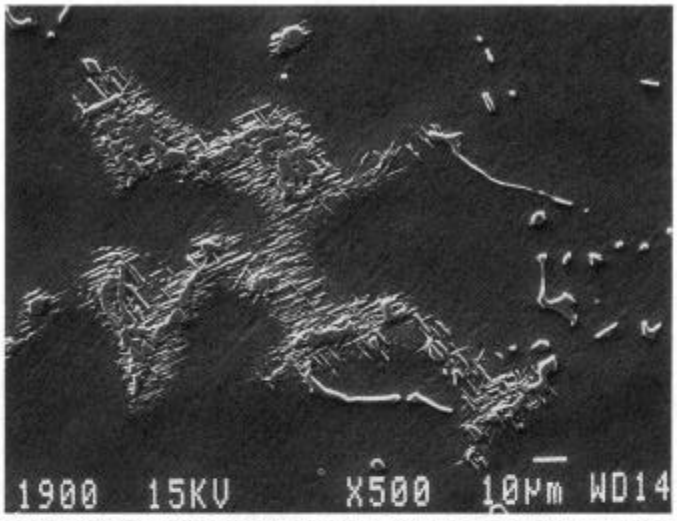

Fig.6 Microstructure of cast alloy 718 after heat treatment at 1037°C/1hr + 927°C/1hr + 927°C/1hr

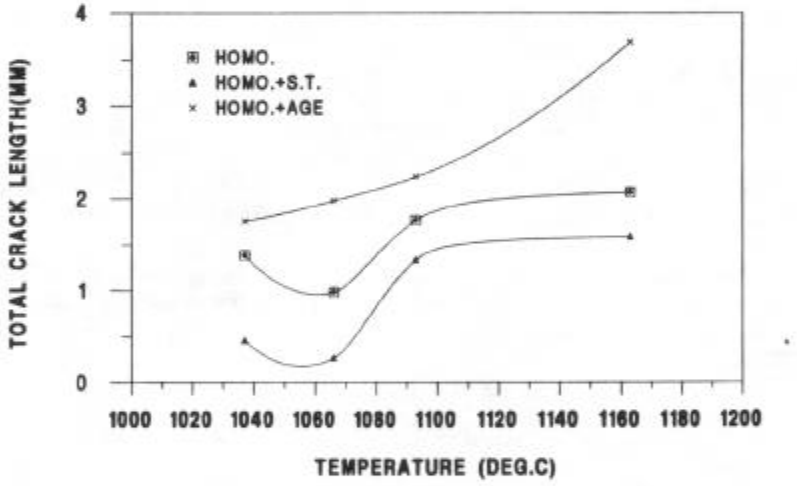

Fig.7 Effect of homogenization, solution and ageing heat treatments on TCL

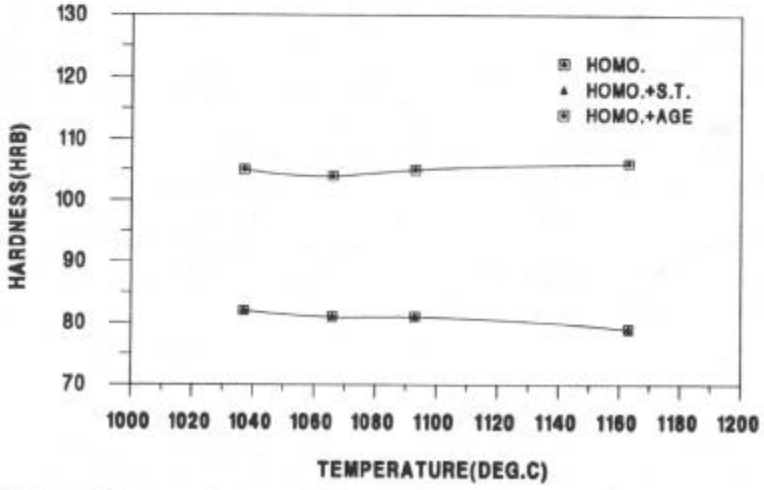

Fig.8 Effect of homogenization, solution and ageing heat treatments on hardness

No apparent microstructural change was observed in SEM after ageing. However it is known that γ" and γ' precipitate during aging which leads to hardness changes. The hardness changes after various heat treatment is described in a subsequent section.

Evaluation of HAZ Microfissuring(TCL)

The values of TCL after various heat treatments were measured, and plotted against the heat treatment temperature as shown in Fig.7. It is observed that the total crack length decreases initially with an increase in the homogenization temperature (1037°C to 1066°C) and then increases over the range of 1066°C to 1163°C.

The TCL after homogenization and solution treatment were determined and are also shown in Fig.7. A trend similar to that seen in homogenized samples was observed, i.e., with increasing homogenization temperature, the TCL decreased (from 1037°C+ST to 1066°C+ST) and then increased (from 1066°C+ST to 1163°C+ST).

The TCL after homogenization and ageing treatments increased as homogenization treatment temperature increased from 1037°C to 1163°C. No minimum in the TCL/temperature curve was found as shown in Fig.7.

Hardness Variation after Various Heat Treatment

As shown in Fig.8, the hardness after homogenization and solution heat treatment has similar values, while higher hardness was obtained after ageing; in addition the hardness values increased with homogenization temperature.

Discussion

Development of Microstructures

The microstructural examination revealed that the volume fraction of δ-Ni_3Nb precipitates decreased with increasing homogenization temperature (Fig.5a) and the precipitates were completely dissolved after 1093°C/1hr. The volume fraction of Laves phase (Fig.5b) showed the same trend as that of the δ phase, with most of the Laves phase going into solution after 1163°C/1hr. The volume fraction of M(C,N) precipitates (Fig.5c) was observed to remain constant through all the various heat treatments used in this study.

Solution heat treatment increased the amount of both intra- and inter-granular precipitates of δ-Ni_3Nb as illustrated in Fig.5a. It has been noted by other researchers[14] that grain boundaries in the interdendritic region associated with δ precipitates showed extensive migration and the uniformly spaced δ plates grew into only one of the adjoining grains. This was confirmed in the present study. The amount of M(C,N) did not change with the solution treatment. Depending on the cooling rate from solution heat treatment, γ" and γ' may precipitate during cooling.

Due to the precipitation of γ" + γ', the hardness (strength) level increased as shown in Fig.8. The γ'+γ" precipitates were not resolved in this study. It was also found by other researchers[15] that δ-Ni_3Nb had grown at the grain boundaries by a discontinuous precipitation mechanism in cast 718 after ageing.

HAZ Microfissuring

In HAZ microfissures were found on solute-enriched grain boundaries adjacent to the fusion zone. Many cast alloys are susceptible to intergranular liquation cracking due to the formation of incipient intergranular liquid films which can cause intergranular cracks. Previous studies on cast alloy 718 showed that both NbC[16,17] and Laves phases [18,19] produce intergranular liquid films when the material in the HAZ experiences rapid thermal cycles during the welding process. It was also theorized that the liquation process is not in itself a sufficient condition to produce severe liquation cracking, but the liquation must also be accompanied by a grain boundary wetting phenomena. One of the factors which can encourage the liquation and wetting is the interaction of elements like boron[20], sulphur[21], phosphorous[22] and carbon[21,23] within the grain boundaries.

The mechanical stresses leading to formation of HAZ cracks arise from the temperature gradients and the difference in thermal expansion in different areas and the resulting plastic deformation associated with the movement of liquid metal zone along the weld and its temperature profile[24]. Evolution of the stresses can depend significantly on the welding parameters, the degree of mechanical constraint associated with the workpiece geometry and weld fixturing, and the thermal properties of the material being welded. The requirements for a liquation crack to form can be summarized as follows:

(1)Formation of liquid on grain boundary
(2)Wetting of the liquid along the grain boundary
(3)Development of thermal stresses

Effect of homogenization Treatment on TCL After Homogenization Treatment: As shown in Fig.7, the TCL-homogenization temperature curve has a U shape. The amount of secondary phases (such as Laves, δ and MC) and hardness values, shown in Fig.5 and 8, respectively, did not vary with the homogenization temperature in the same fashion as the TCL. The existing theories proposed by other investigators, e.g., grain boundary film formation during heat treatment, sulphur segregation to grain boundary and boride decomposition, can not explain the variation in TCL with homogenization temperature. A reasonable interpretation can be provided by the analysis of the results of boron segregation data, determined by SIMS analysis, on the basis of the concepts of equilibrium and non-equilibrium segregation of boron[25]. The variation in the amount of boron segregation with temperature has the same trend as TCL, which suggests that boron segregation to the grain boundary could be contributing to the TCL. Further SIMS analysis carried out on welded specimen revealed strong boron segregation on HAZ microfissures[26]. It is thus concluded that boron plays a significant role in the HAZ microfissuring in this alloy.

The effect of boron segregation on weldability can be explained as follows: a)Boron changes the grain boundary interfacial energy, which increases the wettability of the liquid produced during welding, and b)Boron lowers the solidus of the liquid formed during welding which influences the ability of the grain boundary to accommodate residual stresses occurring during the cooling cycle.

Effect of Homogenization Temperature on TCL after Homogenization and Solution treatment: As discussed in the last section, the TCL increased initially and then decreased as the homogenization temperature increased (Fig.7). The same trend was observed in the homogenized and solution treated samples, but with lower TCL values. The quantitative analysis of secondary phases showed that the increasing homogenization temperature led to a reduction of both inter and intra-granular δ-Ni_3Nb precipitates (Fig.5a). If the precipitation of δ-Ni_3Nb on grain boundaries contributes to the decrease in TCL, an increase in TCL with homogenization temperature should be expected since the amount of δ-Ni_3Nb decreases with homogenization temperature. Also, with an increase in homogenization temperature, more solutes, such as P, S, C and B become available in the matrix which gives rise to segregation during solution treatment. This again causes the TCL to increase with homogenization temperatures. However, neither of the above factors can be used to explain the occurrence of a minimum in TCL-homogenization curve that occurs at 1066°C. Since an extensive investigation has not been carried out regarding elemental segregation and grain boundary microstructural changes after solution treatment, a conclusive explanation can not be given at present.

Effect of Homogenization Temperature on TCL After Homogenization and Ageing Treatment: It is observed in Fig.7 that the TCL tends to increase with homogenization temperature after homogenization and ageing treatment. This could be due to the availability of more solutes in the matrix after the homogenization treatment. With an increase in the homogenization temperature, more solutes such as S, P, C and B, are likely to be released due to the dissolution of precipitates, and from interfaces and interdendritic areas. Since the equilibrium segregation concentration (during the last stage of ageing at 650°C, the extent of non-equilibrium segregation is negligible) is proportional to the solute concentration in the matrix, i.e. $C_b \propto C_m$, a higher grain boundary segregation could be achieved due to the increase in homogenization temperature. As discussed in our previous communication[26], increased grain boundary segregation will assist the formation of HAZ microfissuring and result in higher value of TCL.

Conclusion

1. The microstructure of as-cast alloy 718 consists of γ-matrix, M(C,N), δ-Ni_3Nb, and lamellar Laves phase.

2. The volume fraction of δ-Ni_3Nb and Laves phases was found to decrease with the increasing homogenization temperature, while the amount of M(C,N) did not change when the specimens were heat treated at temperatures up to 1163°C. Solid solution treatment after homogenization enhanced the precipitation of δ-Ni_3Nb. The ageing treatment did not change the amount of Laves phase and M(C,N).

3. The hardness values after homogenization and solid solution treatments have similar values as in the as-cast condition, while ageing increased the hardness due to the precipitation of γ"+γ'.

4. Over the 1037°C to 1163°C range of homogenization temperature, HAZ TCL decreased initially with the homogenization temperature (from 1037°C to 1066°C) and then increased. The TCL after homogenization and solid solution treatment varied in a similar manner with homogenization temperature. The TCL after homogenization + ageing increased with homogenization temperature with no minimum in TCL value observed.

5. The weldability of this alloy after homogenization treatment was found to be closely related to boron grain boundary segregation, i.e. the variation in HAZ TCL with pre-welding heat treatment temperatures has a similar trend as exhibited by the boron segregation with temperature after air cooling.

6. If welding is to be carried out in solution treated condition, a pre-homogenization heat treatment at 1066°C would be beneficial; However, welding if is to be carried out in aged condition, a low homogenization temperature and an intermediate solid solution treatment temperature should be used to minimize the HAZ microfissuring.

Acknowledgement

The authors would like to thank Natural Science and Engineering Research Council of Canada for the financial support through their Research Partnership program.

References

[1] R.G. Carlson and J.F. Radavich, Superalloy 718-Metallurgy and Applications, Ed. E.A. Loria, (1989), P.79.
[2] D.S. Duvall and W.A. Owczarski, Welding Journal, 46(1967), P.423s.
[3] R.G. Thompson, et al. Welding Journal, 4(1985), P.91s.
[4] W.A. Baselack III and D.E. Nelson, Metallography, 19(1986), P.371.
[5] R.G. Thompson, B. Radhakrishnan and D.E. Mayo, J. De Physique, C5, T-49, Oct.(1988), P.471(1988).
[6] R.G. Thompson, J. of Metals, July(1988), P.44.
[7] T. Kelly, Advances in Welding Science and Technology, Ed. S.A.David, (1986), P.623.
[8] T. Kelly, Welding Journal 2(1989), P.44s.
[9] N.L. Richards, X. Huang and M.C. Chaturvedi, Materials Characterization, 28(1992), P.179.
[10] P. Adam, in High Temperature Alloys for Gas Turbines, ed. D. Coutsouradis, (Applied Science Publishers Ltd., London, 1979), P.737.
[11] X. Huang, M.C.Chaturvedi and N.L. Richards, Proceedings of the Third International SAMPE Metals and Materials Processing Conference, Oct. 20-23, Toronto, (1992), p.445.
[12] J.f. Radavich, Journal of Metals, July(1988), P.42.
[13] M.C. Flemings, Solidification Processing, (McGraw-Hill Book Co., NY, 1974), P.31-87.
[14] G. Mrualipharan, R.G. Thompson and S.D. Walck, Proceeding of the Second Conference on Frontiers of Electron Microscopy in Materials Science, May(1989), P.277.
[15] G. Muralidharan and R.G. Thompson and S.D. Walck, Ultramicroscopy, 29(1989), P.277.
[16] R. Vincent, Acta Metall., Vol.33, No.7(1985), P.1205
[17] R.G. Thompson and S. Genculu, Welding Journal, Dec.(1983), P.337s.
[18] W.A. Baselack III and D.E. Nelson, Metallography, 19(1986), P.371.
[19] B. Radhakrishnan and R.G. Thompson, Metallography, Vol.21(1988), P.453.
[20] T. Kelly, Int. Welding Research Conf., ASM, Gatlinburg, TN, 1986.
[21] R.G. Thompson, B. Radhakrishnan, and D.E. Mayo, J. De. Physique, C5, supplement No.10, Tome 49, Oct.(1988), c5-471.
[22] W.F. Savage, E.F.Nippes and G.M. Goodwin, Welding Journal, Aug.(1977), P.245s.
[23] R.G. Thompson, D.E. Mayo and B. Radhakrishnan, Met. Trans. A, Vol.22A, Feb.(1991), P.557.
[24] K. Easterling, in Introduction to the Physical Metallurgy of Welding, (Butterworths, London, 1983), P.1-47.
[25] X. Huang, N.L. Richards and M.C. Chaturvedi, to be published.
[26] X. Huang, Ph.D Dissertation, University of Manitoba, 1994.